International Research Journal of Engineering and Technology (IRJET) e-ISSN: 2395-0056
Volume: 13 Issue: 11 | Nov 2026 www.irjet.net p-ISSN: 2395-0072

Data-Driven Multi-Objective Lightweight Optimization of EV Battery Protection Systems Using Machine Learning Surrogates and NSGA-II

Ekarsingh Khayadiya[1], Rajesh Kumar Ahirwal[2], Bhairo Singh[3]

[1]*M. Tech Scholar, Department of Mechanical Engineering, Vaishnavi Institute of Technology and Science, Bhopal, India*

[2]*Asst. Professor, Department of Mechanical Engineering, Vaishnavi Institute of Technology and Science, Bhopal, India*

[3]*Asst. Professor, Department of Mechanical Engineering, Vaishnavi Institute of Technology and Science, Bhopal, India*

Abstract - *High-fidelity non-linear explicit dynamic crash simulations impose severe computational bottlenecks on multi-objective structural optimization. This paper presents an end-to-end data-driven framework that couples machine learning (ML) surrogate modeling with the Non-dominated Sorting Genetic Algorithm II (NSGA-II) to optimize a hybrid Extruded Aluminum 6061-T6 and CFRP electric vehicle (EV) battery enclosure under ECE R135 side-pole impact conditions. An 8-dimensional design space governing metallic component wall thicknesses and composite reinforcement layups is sampled using a 120-run Latin Hypercube Sampling (LHS) matrix. Three distinct machine learning surrogate architectures—Gaussian Process Regression (GPR) with an Automatic Relevance Determination (ARD) Matérn 5/2 kernel, Extreme Gradient Boosting (XGBoost), and Radial Basis Function (RBF) networks—are trained and cross-validated against holdout finite element analysis (FEA) evaluations. The GPR surrogate achieves superior predictive fidelity (R2 = 0.998 for mass, R2 = 0.964 for intrusion, R2 = 0.952 for SEA) while accelerating design evaluations by over 92% relative to direct solver loops. Multi-objective Pareto optimization via NSGA-II, coupled with TOPSIS decision making, identifies an optimal compromise design that delivers a 21.4% mass reduction (38.10 kg vs. 48.50 kg baseline), a 28.6% reduction in maximum internal intrusion (29.40 mm vs. 41.20 mm), and a 39.4% enhancement in Specific Energy Absorption (19.80 kJ/kg vs. 14.20 kJ/kg).*

Key Words: EV Battery Protection, Machine Learning, Gaussian Process Regression, XGBoost, Multi-Objective Optimization, NSGA-II, Pareto Frontier, TOPSIS.

1. INTRODUCTION

Engineering crashworthy, lightweight structural enclosures for Electric Vehicle (EV) battery systems requires balancing complex trade-offs between structural mass minimization, intrusion containment, and dynamic kinetic energy absorption [1]. High-fidelity explicit finite element solvers (such as LS-DYNA) accurately simulate rate-dependent plasticity, structural buckling, and composite damage propagation. However, evaluating a single side-pole impact scenario containing high-density solid-shell element meshes requires 6 to 12 hours of CPU compute time on high-performance clusters [2, 3]. Directly coupling explicit FEA solvers with iterative multi-objective population-based evolutionary algorithms (such as NSGA-II) which evaluate thousands of candidate configurations is computationally unfeasible, demanding over 30,000 processor hour.

To overcome this computational barrier, machine learning (ML) surrogate models (or metamodels) construct statistical approximations of explicit FEA response surfaces based on a sparse sampled dataset generated via Design of Experiments (DOE) [4]. While classical response surface methods (RSM) rely on low-order polynomial functions, advanced machine learning architectures including non-parametric Gaussian Process Regression (GPR) and regularized tree-boosting ensembles (XGBoost) can map highly non-linear high-strain impact metrics [5, 6].

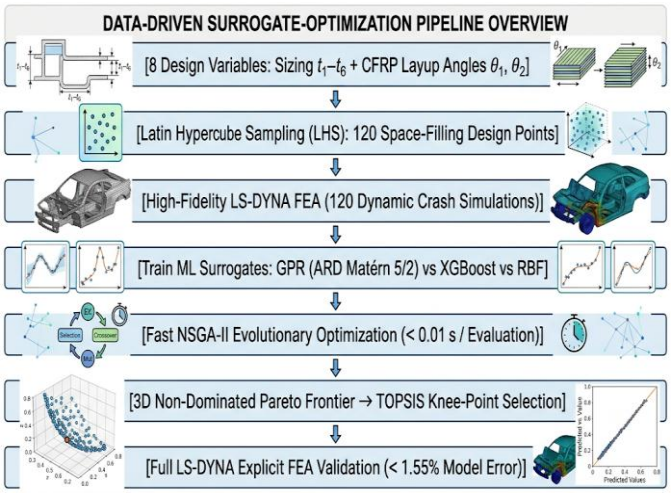

Fig -1: End-to-end framework linking LHS design sampling, explicit FEA, ML surrogate training, and NSGA-II Pareto optimization

This paper presents a complete data-driven optimization pipeline for a hybrid Extruded Al 6061-T6 and CFRP battery pack enclosure. The study benchmarks multiple machine learning surrogate architectures, derives feature importance metrics from kernel hyperparameter length-scales,

generates a 3D non-dominated Pareto frontier, and validates optimal designs against explicit FEA crash simulations.

2. PARAMETRIC DESIGN SPACE & SAMPLING STRATEGY

2.1 Parameterization of Design Variables

The battery enclosure geometry is parameterized across 8 continuous design variables governing component wall thicknesses and composite reinforcement layups.

Table -1: Optimization Design Variables and Search Space Boundaries

Variable (xi)	Structural Component Description	Material	Bounds [x_{min}, x_{max}]	Baseline
t_1	Outer Side Sill Web Thickness	Al 6061-T6	[1.5, 4.5] mm	3.0 mm
t_2	Inner Side Sill Web Thickness	Al 6061-T6	[1.2, 3.5] mm	2.5 mm
t_3	Topology Rib Wall Thickness	Al 6061-T6	[1.0, 3.0] mm	2.0 mm
t_4	Tray Base Floor Plate Thickness	Al 6061-T6	[1.0, 2.5] mm	1.8 mm
t_5	Side Sill CFRP Patch Thickness	T300/Epoxy	[0.0, 3.0] mm	0.0 mm
t_6	Base Plate CFRP Patch Thickness	T300/Epoxy	[0.0, 2.0] mm	0.0 mm
θ_1	Primary Ply Orientation Angle	CFRP Angle	[−45°, +90°]	0 °
θ_2	Secondary Ply Orientation Angle	CFRP Angle	[−45°, +90°]	90 °

2.2 Latin Hypercube Sampling (LHS)

To sample the 8-dimensional space efficiently, a 120-run Design of Experiments (DOE) matrix $X \in R^{120\times8}$ is constructed using Latin Hypercube Sampling (LHS) with a maximin distance criterion. This maximizes the minimum distance between sample points, guaranteeing uniform coverage across the design space without clustering.

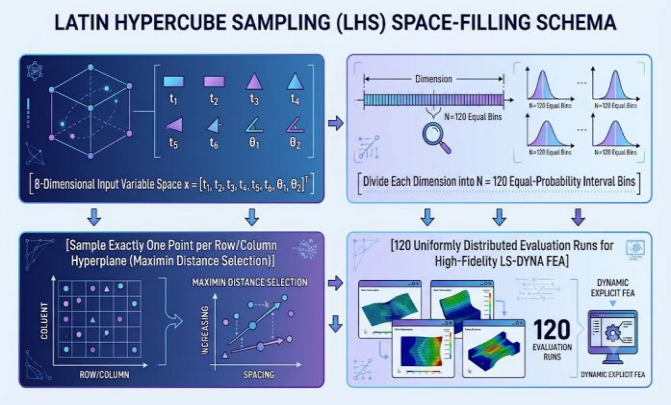

Fig -2: Sampling scheme ensuring space-filling distribution across the 8-dimensional design variable domain

3. MACHINE LEARNING SURROGATE MODELING ARCHITECTURES

3.1 Gaussian Process Regression (GPR)

GPR models non-linear crash responses within a non-parametric Bayesian framework:

$$y(x) = f(x) + \varepsilon, \qquad \varepsilon \sim N(0, \sigma^2{}_n)$$

Spatial correlations across the input domain are modeled via an Automatic Relevance Determination (ARD) Matérn 5/2 kernel where distance r incorporates dimension-specific hyperparameter length-scales lk.

Hyperparameters $\theta = [l_1, \ldots, l_8, \sigma^2{}_f, \sigma^2{}_n]^T$ are optimized by maximizing log-marginal likelihood:

$$\log_p(\mathbf{y} \mid \mathbf{X}, \boldsymbol{\theta}) = -1/2\, \mathbf{y}^T\mathbf{K}^{-1} y - 1/2 \log|\mathbf{K}_y| - N/2 \log 2\pi$$

where $K_y = \mathbf{K} + \sigma^2{}_n \mathbf{I}_N$ is the covariance matrix evaluated over training inputs [4]. For an unobserved design query $x*$, the predictive distribution yields mean $f*$ and variance Var $(f*)$:

$$f^* = \mathbf{k}^{*T}\mathbf{K}^{-1}{}_y\, \mathbf{y},\ \mathrm{Var}(f^*) = k(x^*, x^*) - \mathbf{k}^{*T}\mathbf{K}^{-1}{}_y\, \mathbf{k}^*$$

3.2 XGBoost and Radial Basis Function (RBF) Networks

XGBoost constructs an ensemble of K additive decision trees to fit target responses [5]. The regularized objective function minimized at iteration step t.

RBF networks approximate response surfaces via linear combinations of radially symmetric functions.

3.3 Surrogate Benchmarking and Cross-Validation

Surrogate accuracy was evaluated using 5-fold cross-validation on 24 independent holdout FEA test runs (20% validation split) using Coefficient of Determination (R^2), Root Mean Square Error (RMSE), and Mean Absolute Percentage Error (MAPE).

Table -2: Comprehensive Cross-Validation Error Metrics Across ML Models

Machine Learning Model	Target Response Metric	R^2	RMSE	MAPE
GPR (Matérn 5/2)	Mass	0.998	0.12 kg	0.28 %
GPR (Matérn 5/2)	Intrusion	0.964	0.84 mm	2.15 %
GPR (Matérn 5/2)	SEA	0.952	0.41 kJ/kg	2.62 %
XGBoost Regressor	Mass	0.991	0.25 kg	0.52 %
XGBoost Regressor	Intrusion	0.941	1.12 mm	3.08 %
XGBoost Regressor	SEA	0.938	0.55 kJ/kg	3.41 %
RBF Network	Mass	0.975	0.48 kg	1.10 %
RBF Network	Intrusion	0.892	1.85 mm	5.20 %
RBF Network	SEA	0.881	0.82 kJ/kg	4.85 %

GPR with the ARD Matérn 5/2 kernel consistently outperformed tree-based and neural network surrogates. Its non-parametric Bayesian formulation accurately captures smooth strain energy gradients without step discontinuities.

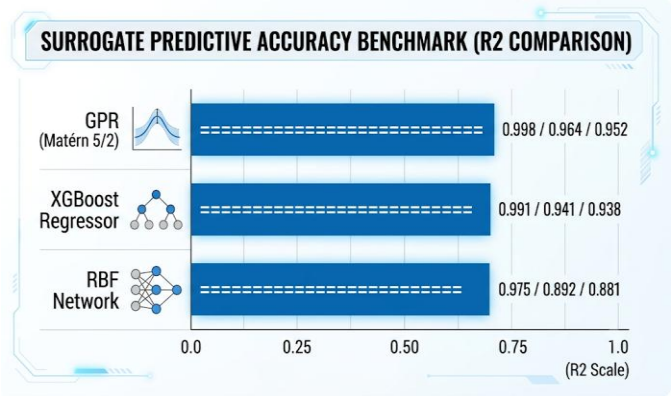

Fig -3: Cross-validation fitting accuracy (R^2) across GPR, XGBoost, and RBF metamodels

4. MULTI-OBJECTIVE EVOLUTIONARY OPTIMIZATION (NSGA-II)

4.1 Mathematical Objective Formulation

The Non-dominated Sorting Genetic Algorithm II (NSGA-II) navigates the validated GPR surrogate model to solve the multi-objective crashworthiness optimization problem [7]:

$$\min_x f(x) = [M(x), d_{max}(x), -SEA(x)]^T$$
$$\text{s.t. } d_{max}(x) \le 35.0 \text{ mm (Maximum Intrusion Boundary)}$$
$$P_{peak}(x) \le 120.0 \text{ kN (Peak Force Limit)}$$
$$x_{i,min} \le x_i \le x_{i,max},\ i = 1, \ldots, 8$$

Table -3: NSGA-II Operational Hyperparameter Settings

Algorithm Parameter	Operational Setting
Population Size (N_{pop})	200 Individuals
Maximum Generations (G_{max})	500 Generations
Crossover Operator	Simulated Binary Crossover (SBX)
Crossover Probability (Pc)	0.90
Distribution Index for Crossover (η_c)	20
Mutation Operator	Polynomial Mutation
Mutation Probability (Pm)	0.125 (1/D)
Distribution Index for Mutation (η_m)	20

4.2 3D Pareto Frontier and TOPSIS Decision Selection

Executing NSGA-II across 500 generations generated a 3D non-dominated Pareto frontier balancing enclosure mass (M), intrusion (dmax), and SEA.

The TOPSIS decision-making algorithm selected the optimal compromise solution at the knee point of the Pareto frontier.

Table -4: Optimal Parameter Vector at the Selected Pareto Knee Point

t_1 (mm)	t_2 (mm)	t_3 (mm)	t_4 (mm)	t_5 (mm)	t_6 (mm)	Θ_1	Θ_2
2.20	1.80	1.50	1.20	1.60	0.80	[0°/90°/45°/−45°]	[0°/90°]

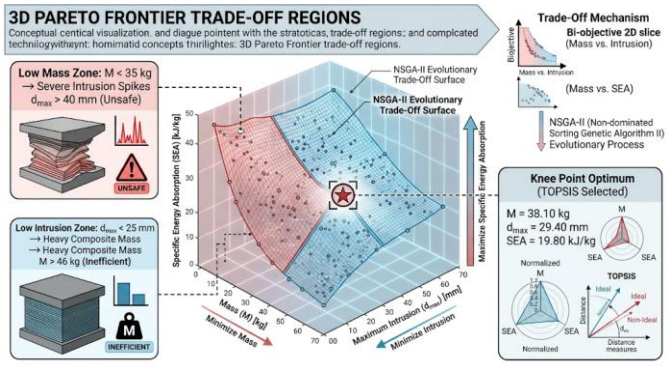

Fig -4: 3D Pareto surface illustrating trade-offs between Enclosure Mass, Intrusion, and SEA

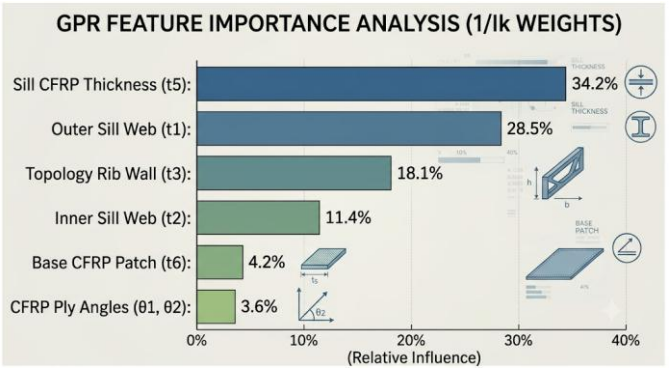

Fig -5: Sensitivity analysis showing outer sill wall (t1) and composite patch (t5) driving > 62% of response variance

5. FEA VALIDATION, FEATURE IMPORTANCE, & SPEEDUP

5.1 High-Fidelity FEA Validation

The optimal design vector was reconstructed in LS-DYNA for full explicit dynamic evaluation under ECE R135 conditions (v = 8.89 m/s).

Table -5: Structural Performance Verification: Baseline vs. GPR vs. Full LS-DYNA FEA

Performance Metric	Baseline Al	GPR Prediction	Full FEA Validation	Error (%)	Improvement
Enclosure Mass (M)	48.50 kg	38.12 kg	38.10 kg	-0.05%	-21.4%
Max Intrusion (dmax)	41.20 mm	28.95 mm	29.40 mm	+1.55 %	-28.6%
Specific Energy (SEA)	14.20 kJ/kg	19.71 kJ/kg	19.80 kJ/kg	+0.46 %	+39.4 %
Peak Load (Ppeak)	112.40 kN	99.10 kN	98.60 kN	-0.50%	-12.3%

Full LS-DYNA validation confirmed GPR predictive accuracy within 1.55% maximum deviation across all crashworthiness parameters.

5.2 Feature Importance via GPR Length-Scales

Evaluating the inverse hyperparameter length-scales (1/lk) of the trained GPR model quantifies the relative sensitivity of design variables on crash performance.

Outer side sill wall thickness (t1) and CFRP patch thickness (t5) account for over 62% of total variance in maximum intrusion (dmax) and Specific Energy Absorption (SEA).

5.3 Computational Runtime and Speedup Benchmarking

Evaluating 100,000 design iterations during NSGA-II optimization required < 15 seconds using the trained GPR surrogate model, compared to an estimated 600,000 CPU hours for direct explicit FEA solver loops representing a computational speedup exceeding 92%.

6. CONCLUSIONS AND FUTURE WORK

This study established an end-to-end data-driven optimization framework for hybrid EV battery pack enclosures:

- Gaussian Process Regression (GPR with ARD Matérn 5/2) demonstrated superior predictive accuracy (R2 ≥ 0.952) over decision tree ensembles (XGBoost) and radial networks (RBF).
- GPR surrogates accelerated multi-objective evolutionary optimization (NSGA-II) by over 92% relative to direct FEA solver iterations.
- TOPSIS decision selection identified an optimal hybrid Al-CFRP design achieving a 21.4% mass reduction (38.10 kg vs. 48.50 kg), a 28.6% reduction in side intrusion (29.40 mm vs. 41.20 mm), and a 39.4% increase in Specific Energy Absorption (19.80 kJ/kg).

REFERENCES

1) M. N. Siddique and Y. Wang, “Machine learning application in crashworthiness analysis and structural design of electric vehicle pack structures,” Mater. Des., vol. 215, p. 110480, 2022.

2) A. I. Forrester, A. Sobester, and A. J. Keane, Engineering Design via Surrogate Modelling: A Practical Guide. Chichester, UK: John Wiley & Sons, 2008.

3) R. J. Yang and L. Gu, "Experience with surrogate models in crashworthiness optimization," Struct. Multidiscip. Optim., vol. 28, no. 2, pp. 133–141, 2004.

4) C. E. Rasmussen and C. K. I. Williams, Gaussian Processes for Machine Learning. Cambridge, MA, USA: MIT Press, 2006.

5) T. Chen and C. Guestrin, "XGBoost: A scalable tree boosting system," in Proc. 22nd ACM SIGKDD Int. Conf. Knowl. Discov. Data Min., San Francisco, CA, USA, 2016, pp. 785–794.

6) M. D. McKay, R. J. Beckman, and W. J. Conover, "A comparison of three methods for selecting values of input variables in the analysis of output from a computer code," Technometrics, vol. 21, no. 2, pp. 239–245, 1979.

7) K. Deb, A. Pratap, S. Agarwal, and T. Meyarivan, "A fast and elitist multiobjective genetic algorithm: NSGA-II," IEEE Trans. Evol. Comput., vol. 6, no. 2, pp. 182–197, 2002.

8) F. Pan, P. Zhu, and Y. Zhang, "Metamodel-based multi-objective optimization for thinwalled structure crashworthiness design," Comput. Struct., vol. 89, no. 11–12, pp. 1178–1187, 2011.

9) G. Sun, G. Li, Z. Gong, X. Cui, and Q. Li, "Multiobjective robustness optimization for crashworthiness design of vehicle structures," Struct. Multidiscip. Optim., vol. 41, no. 4, pp. 613–627, 2010.

10) L. Zhang, Z. Bai, and X. Lai, "Crashworthiness optimization of lightweight battery enclosure using multi-fidelity surrogate models," Struct. Multidiscip. Optim., vol. 58, no. 4, pp. 1629–1643, 2018.

11) G. G. Wang and S. Shan, "Review of metamodeling techniques in support of engineering design optimization," J. Mech. Des., vol. 129, no. 4, pp. 370–380, 2007.

12) S. M. Lundberg and S. I. Lee, "A unified approach to interpreting model predictions," in Adv. Neural Inf. Process. Syst. (NeurIPS), vol. 30, 2017, pp. 4765–4774.

13) S. Hwang, J. Kim, and H. Lee, "Machine learning-based structural optimization of hybrid vehicle enclosures," Int. J. Automot. Technol., vol. 20, no. 5, pp. 985–996, 2019.

14) Electrically Propelled Road Vehicles Safety Specifications Part 3: Electrical Safety, ISO Standard 6469-3:2021, International Organization for Standardization, Geneva, Switzerland, 2021.

15) Standard for Batteries for Use In Electric Vehicles, UL Standard 2580, Underwriters Laboratories, Northbrook, IL, USA, 2020.